

Electronic Supplementary Information

Formation of Quasi-Mesocrystal ZnMn₂O₄ Twin-Microspheres via an Oriented-Attachment for Lithium-Ion Batteries

Yurong Liu, Jing Bai, Xiaojian Ma, and Shenglin Xiong*

[*] Prof. S. L. Xiong, Dr. Y. R. Liu, Dr. J. Bai, Dr. X. J. Ma

Key Laboratory of the Colloid and Interface Chemistry (Shandong University), Ministry of Education, and School of Chemistry and Chemical Engineering, Shandong University, Jinan, 250100, PR China

E-mail: chexsl@sdu.edu.cn (S. L. X.)

Dr. Y. R. Liu

School of Resources and Environmental Engineering, Shandong University of Technology, Zibo, Shandong, 255049, PR China

Prof. S. L. Xiong

CAS Key Laboratory of Materials for Energy Conversion, University of Science and Technology of China, Hefei, Anhui, 230026 (P. R. China)

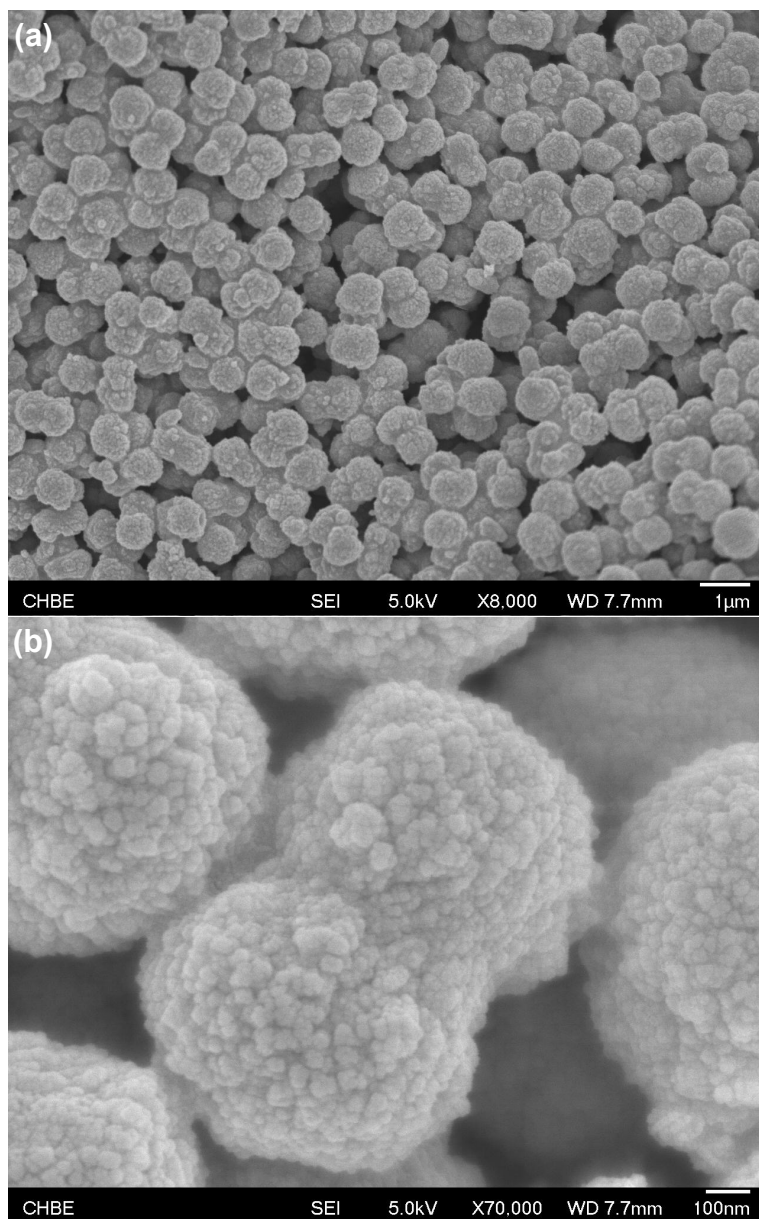


Figure S1. Different magnification FESEM images of $\text{Zn}_{0.33}\text{Mn}_{0.67}\text{CO}_3$ twin-microspheres.

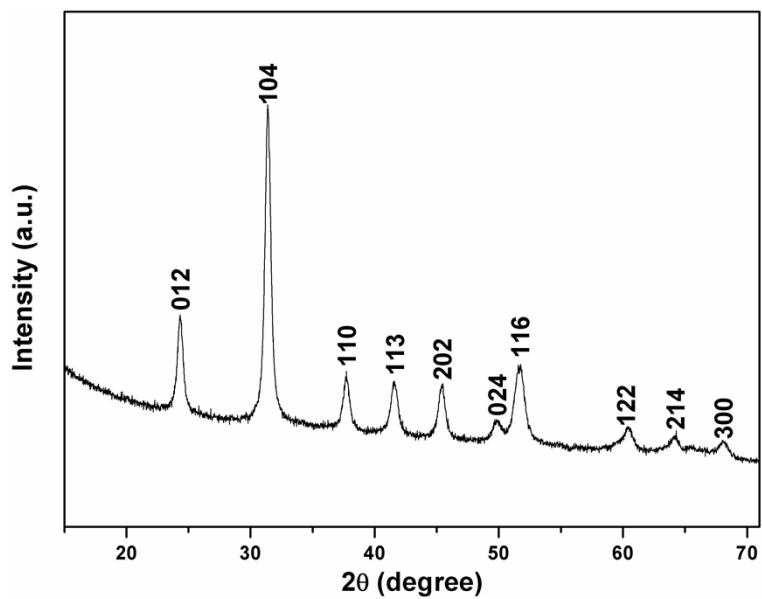


Figure S2. XRD pattern of the $\text{Zn}_{0.33}\text{Mn}_{0.67}\text{CO}_3$ twin-microspheres.

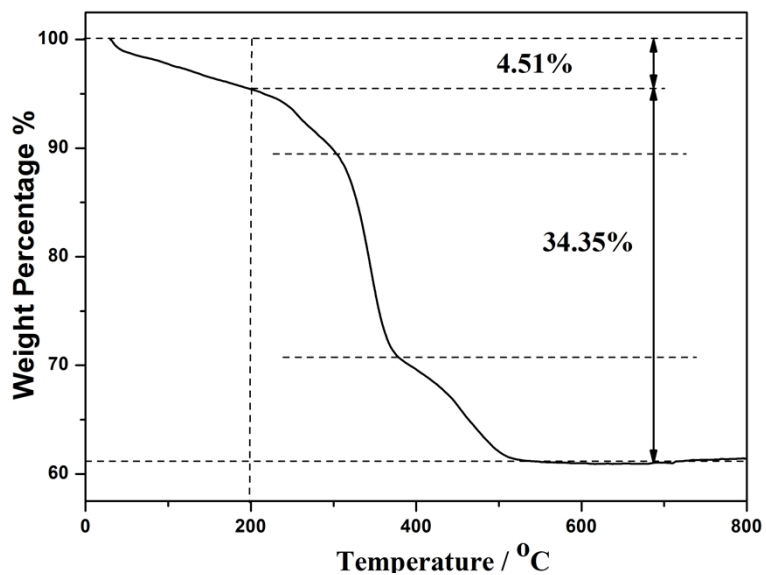


Figure S3. TGA curve of the $\text{Zn}_{0.33}\text{Mn}_{0.67}\text{CO}_3$ twin-microspheres.

Note: The investigations of the thermal behavior of $\text{Zn}_{0.33}\text{Mn}_{0.67}\text{CO}_3$ twin-microspheres by the thermogravimetric analysis (TGA) are displayed in Figure S3, which could be

categorized into two major weight loss steps: the first weight loss below 200 °C is attributed to the loss of physically and chemically adsorbed water, while the second prominent one is due to the thermal decomposition of these solid precursors into ZnMn_2O_4 , and CO_2 in the presence of an air stream used in the TGA measurement. For $\text{Zn}_{0.33}\text{Mn}_{0.67}\text{CO}_3$, the value of the second weight loss is 33.53%, which are slightly larger than the theoretical value (32.67%), possibly due to the presence of tightly bound OH- and/or occluded water molecules and migration of atoms with the exception of CO_2 release during the thermal decomposition. Note that the second major weight loss can also be divided into three steps, as shown in Figure S3 which could originate from the different thermal behaviors of ZnCO_3 and MnCO_3 .

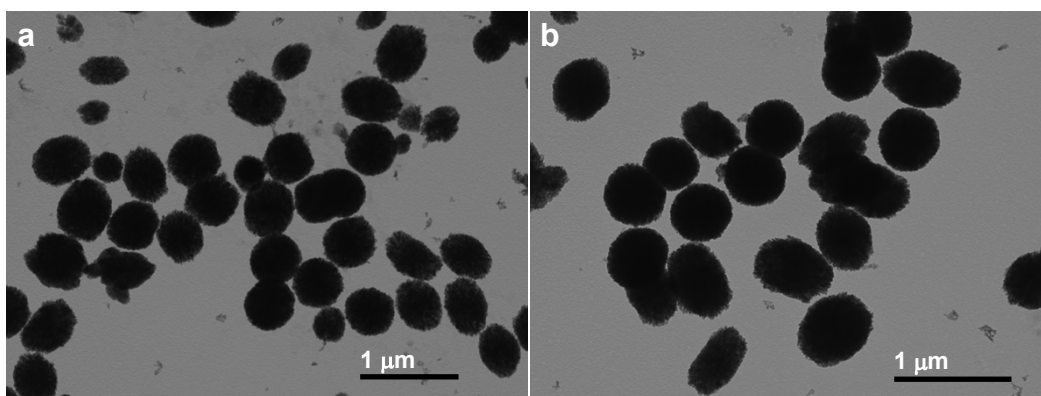


Figure S4. FESEM images of the corresponding precursor samples prepared at 200 °C for 20 h only replacing zinc/manganese acetate with zinc/manganese chloride.

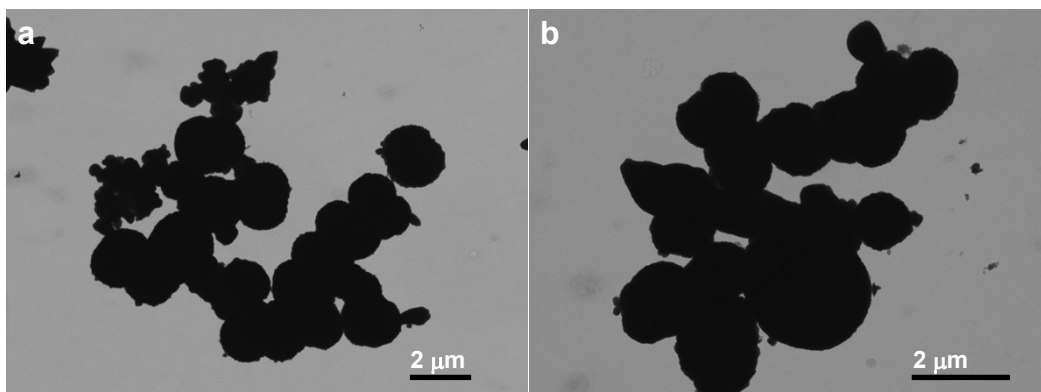


Figure S5. FESEM images of the corresponding precursor samples prepared at 200 °C for 20 h only replacing zinc/manganese acetate with zinc/manganese sulfate.

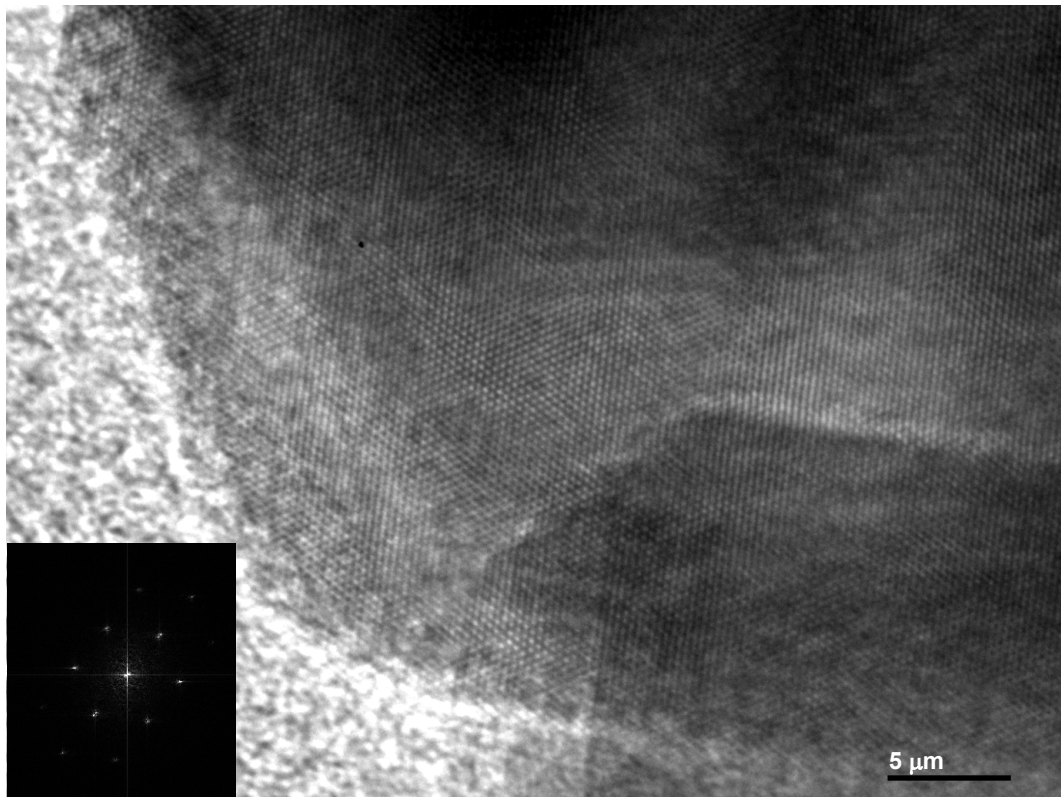


Figure S6. HRTEM image of several small nanoparticles of a ZnMn₂O₄ twin-sphere. The inset is the corresponding FFT-ED pattern.

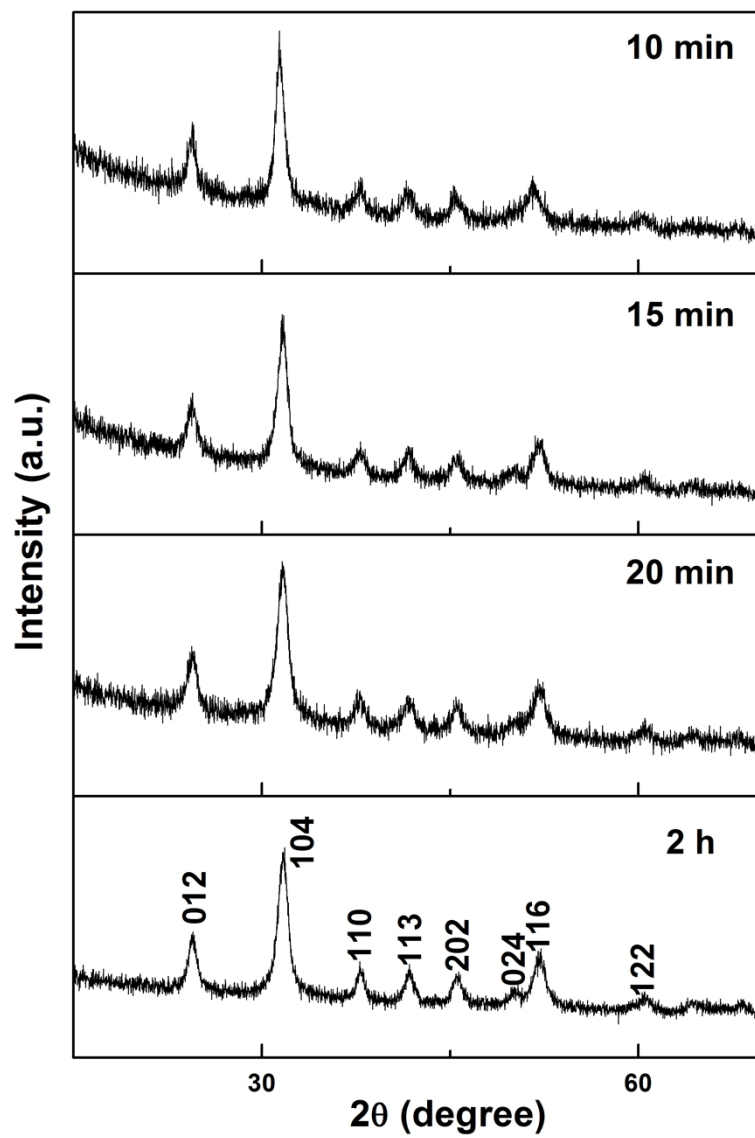
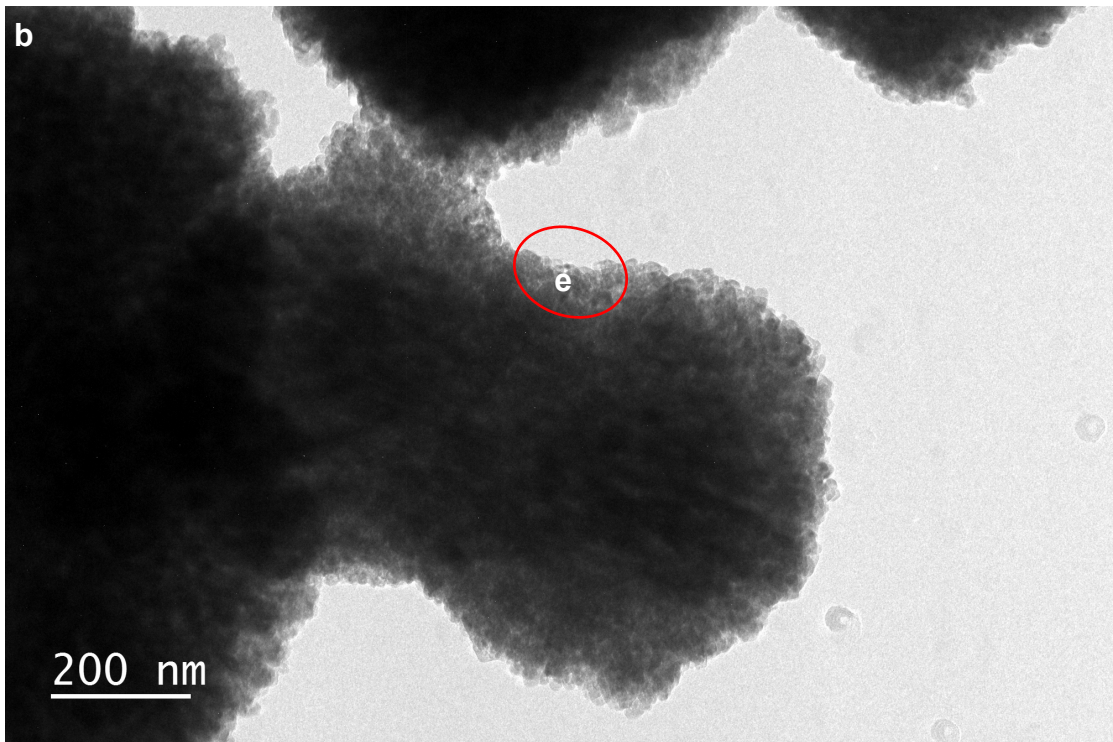
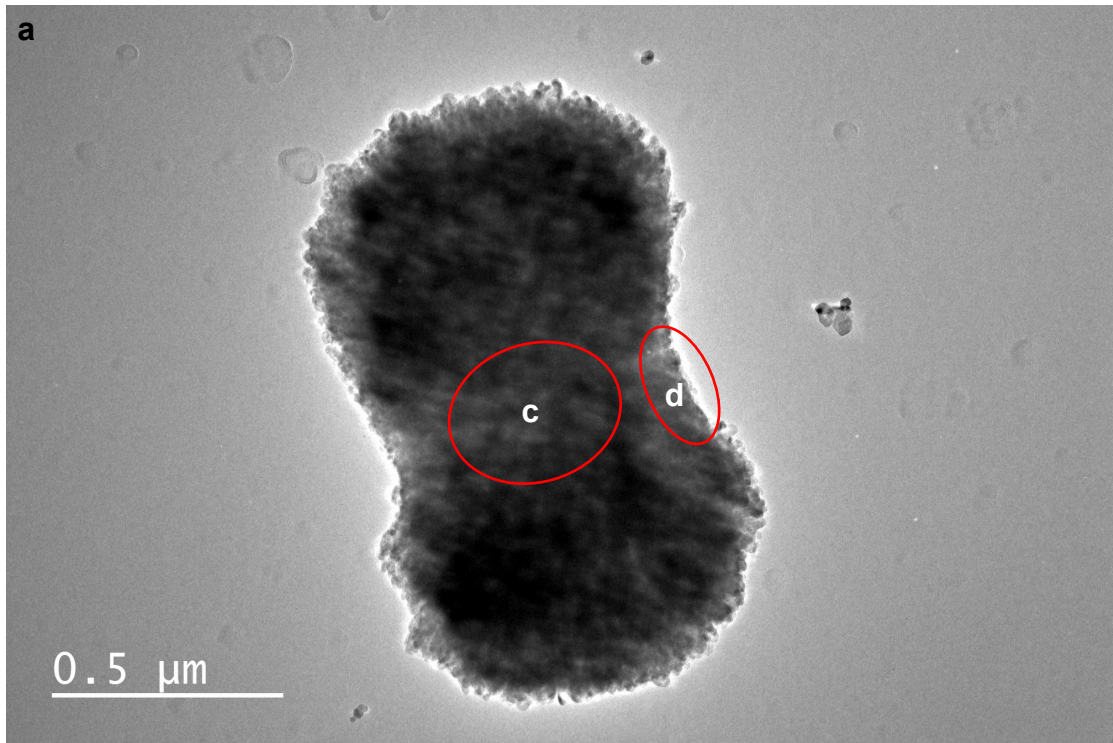
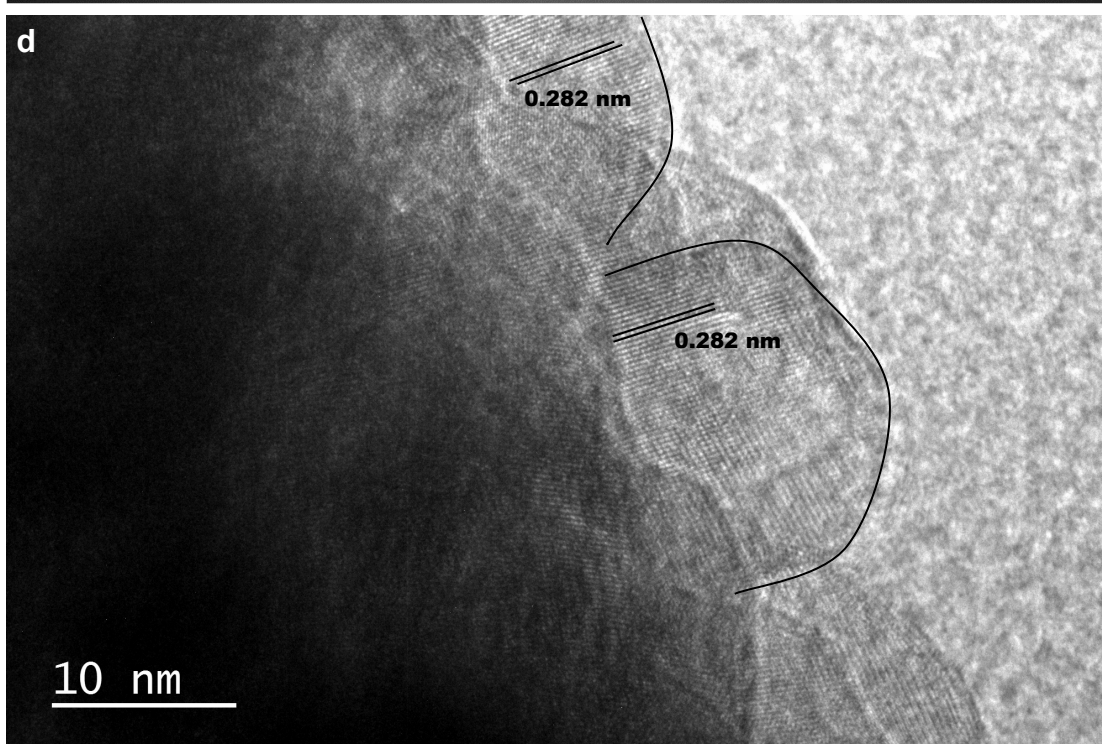
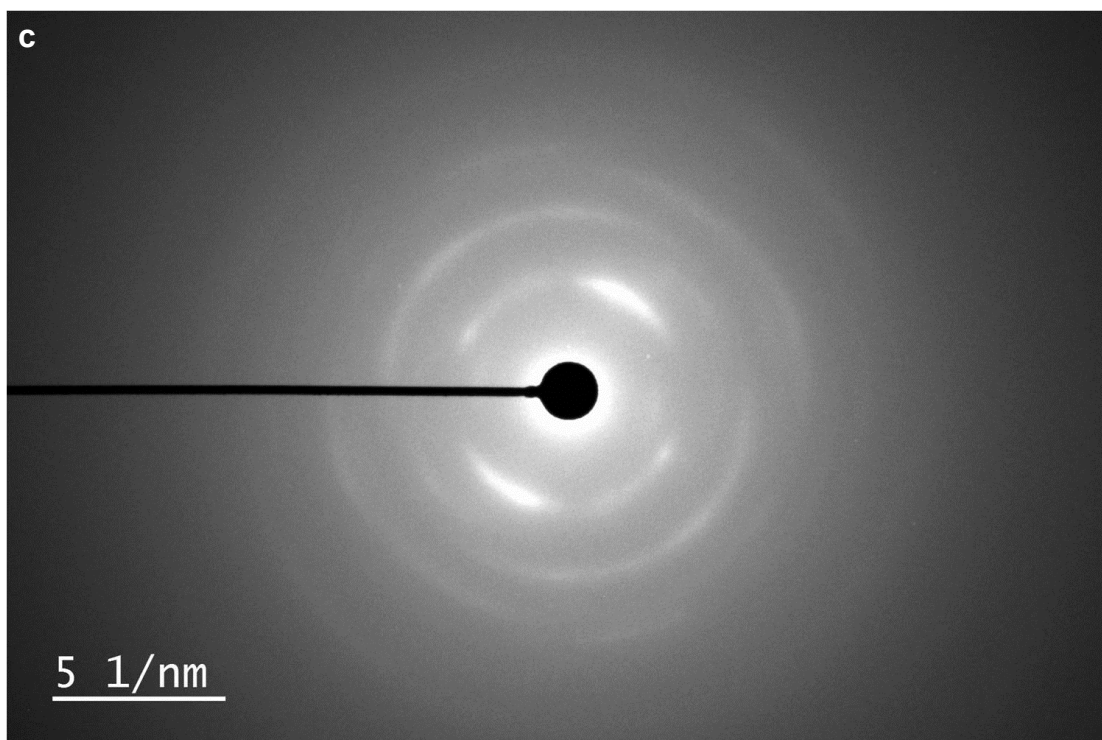


Figure S7. XRD pattern of the corresponding precursor obtained different reaction time.





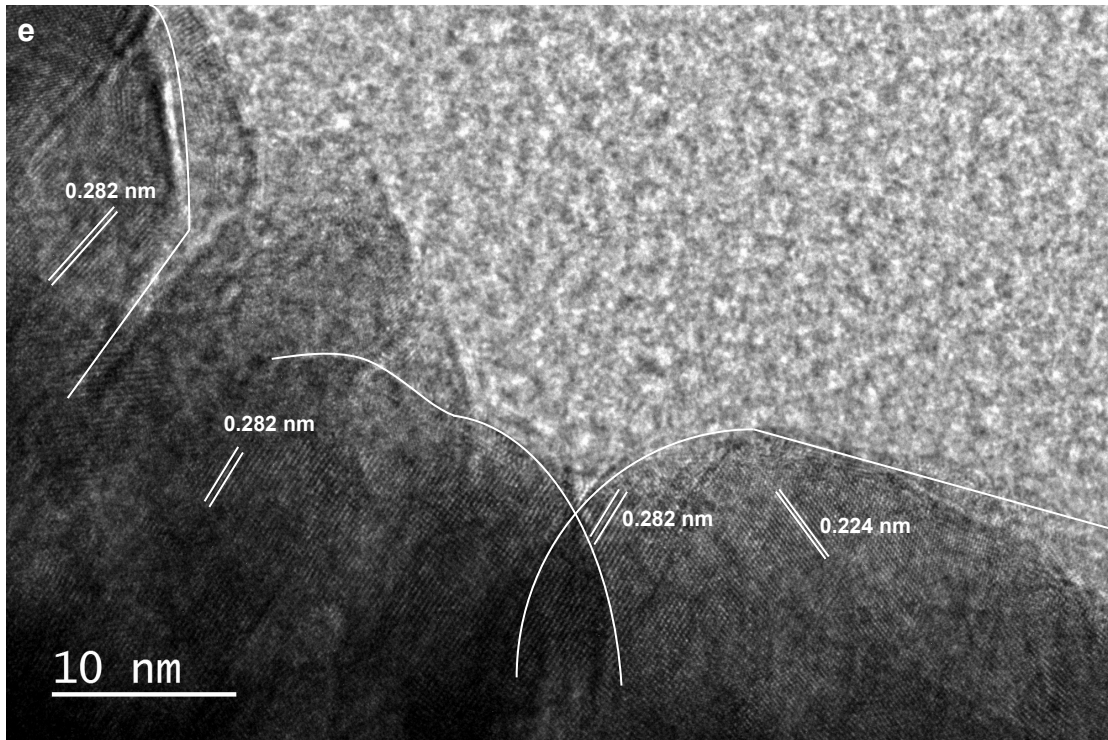


Figure S8. TEM, SAED & HRTEM investigation of $\text{Zn}_{0.33}\text{Mn}_{0.67}\text{CO}_3$ twin-spheres. (a,b) TEM image of a representative $\text{Zn}_{0.33}\text{Mn}_{0.67}\text{CO}_3$ twin-sphere, (c) SAED pattern of (a), and (d) HRTEM image for the area marked in (a), (e) HRTEM image for the area marked in (b).

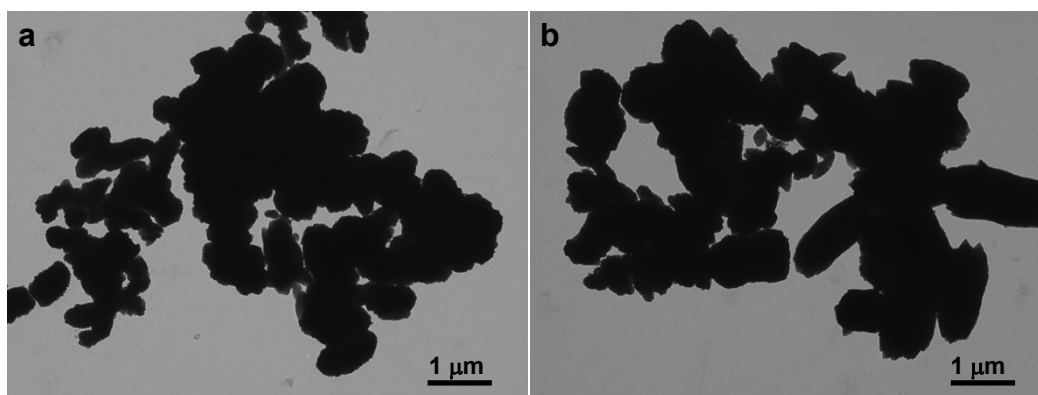


Figure S9. FESEM images of the corresponding precursor samples prepared at 200 °C for 20 h only replacing DEG with ethanol.

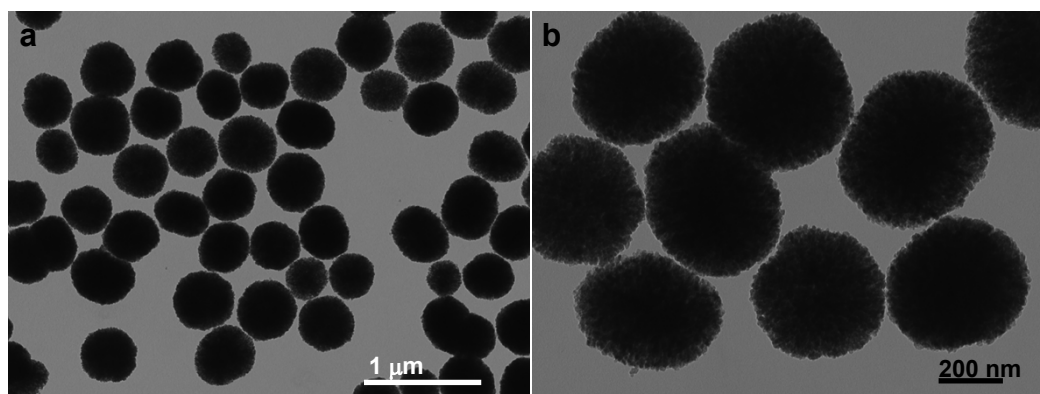


Figure S10. FESEM images of the corresponding precursor samples prepared at 200 °C for 20 h only replacing DEG with EG.

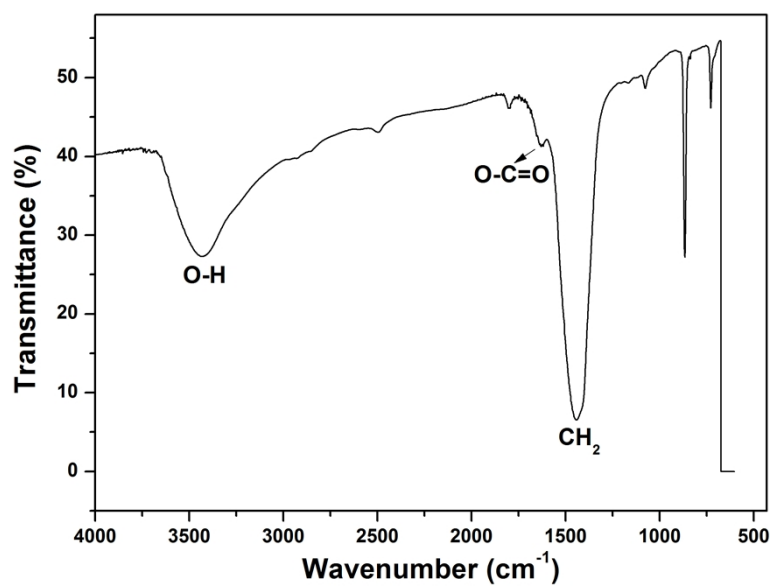


Figure S11. FT-IR spectrum of the corresponding precursor when reaction time is 10 min.